Multiple abnormalities due to a nonsense mutation in the *Alx4* gene

B. Chen[1]*, Lu Chen[2]*, Y. Zhou[3]*, T. Mi[1], D.Y. Chen[1], Li Chen[1], J. Yin[1] and Z.F. Xue[1]

[1]Comparative Medicine Center, Yangzhou University, Yangzhou, China
[2]Sinopharm Group, Yangzhou Vacbio Engineering Co. Ltd., Yangzhou, China
[3]Jiangsu Institute of Cancer Research, Affiliated Cancer Hospital of Nanjing, Medical University, Nanjing, China

*These authors contributed equally to this study.
Corresponding author: Z.F. Xue
E-mail: zfxue@yzu.edu.cn

ABSTRACT. Patterning of the limb anterior-posterior axes depends on several signals that derive from the three signaling centers of the limb bud. These signals interact to constitute a complex and ordered network that critically contributes to the development of limb buds. Preaxial polydactyly in mouse is predominantly caused by ectopic expression of the zone of polarizing activity or Sonic hedgehog in the anterior region of the limb bud. In this study, we describe an *N*-ethyl-*N*-nitrosourea-induced polydactylous mouse (*Alx4^{m1Yzcm}*) with an extra digit on the anterior aspect of one or two hinddigits. The mutation was mapped to chromosome 2, between markers *D2Mit45* and *D2Mit184*. The *Alx4* gene was identified as a potential candidate gene in this location. Sequence analysis of the *Alx4* gene for polydactylous heterozygotes revealed an A/T transversion mutation that resulted in substitution of a lysine codon with a stop (nonsense) codon at position 145. *Alx4^{m1Yzcm}* homozygous mice exhibited multiple abnormalities, including extensive preaxial polydactyly of all four limbs (up to seven digits) and the formation of omphalocele.

Key words: *N*-ethyl-*N*-nitrosourea; Polydactyly; Omphalocele; *Alx4*

INTRODUCTION

During development of vertebrate limbs, patterning is established by the interaction of three different signaling centers: 1) the apical ectodermal ridge (AER), a group of ectodermal cells located at the most distal tip of the limb bud, which permit limb bud elongation along the proximal-distal axes and interact with the zone of polarizing activity (ZPA); 2) the ZPA, a collection of posterior mesenchymal cells, which is considered to direct patterning along the anterior-posterior axes (AP) of the limb; and 3) the dorsal ectoderm, contributing to the formation of dorsal-ventral axes (Catala, 2000; Hu and He, 2008; Tabin and McMahon, 2008).

AER and ZPA are considered essential for the accurate AP patterning. Sonic hedgehog (*Shh*) has been shown to be expressed in the ZPA and mediates polarizing activity. Ectopic expression of *Shh* in the anterior limb also induces digit duplication equivalent to that produced by ZPA grafting (Riddle et al., 1993). Analysis of polydactyly mutations showed that *Shh* transcription is negatively regulated by several genes including *Fgf*, *Gli3*, and aristaless-like 4 (*Alx4*). Deficiency in *Gli3*, which encodes a zinc finger protein that acts as a transcription factor, leads to the extra toes (Xt) mutation, and the *Alx4* is considered to be linked to the mouse mutant Strong's luxoid (*Lst*) (Büscher et al., 1998; Qu et al., 1998; Kuijper et al., 2005; Panman et al., 2005). During limb bud development, *Alx4* becomes critical for repression of anterior ectopic *Shh* expression (Qu et al., 1997).

N-ethyl-*N*-nitrosourea (ENU) is a powerful point mutagen that can generate random mutations in the mouse genome (Chen et al., 2011). In this study, we identified an A/T transition mutation at position 433 of *Alx4*, resulting in the conversion of a lysine codon to a stop (nonsense) codon at position 145 in the protein. The mutant mouse was designated *Alx4*[m1Yzcm] (*Alx4*, mutation 1, Yangzhou University Comparative Medicine Center). Further investigation showed multiple abnormalities in *Alx4*[m1Yzcm] homozygous mice.

MATERIAL AND METHODS

Mice

C57BL/6J (B6) and DBA/2J (D2) mice were obtained from the Shanghai Laboratory Animal Center (Shanghai, China). This study was conducted in strict accordance with the Guide for the Care and Use of Laboratory Animals of the National Research Council. The Animal Care and Use Committee of the Yangzhou University approved all animal experiments and procedures (Approval ID: SYXK [Su] 2012-0029).

The *Alx4*[m1Yzcm] mouse of B6 background was generated by ENU mutagenesis. The *Alx4*[m1Yzcm] heterozygotes were mated to B6 females to confirm the results of the inheritance test. Homozygous mutants were generated by intercross of the heterozygous mutants.

Alcian blue and alizarin red staining

Newborn mice were sacrificed, eviscerated, placed in a 70°C water bath for 30 s, skinned, and then fixed in 100% ethanol for 3 days. The fixed samples were stained with alcian blue (15 mg in 80 mL ethanol/20 mL glacial acetic acid) for 8-12 h. The skeletons were rinsed in 100% ethanol overnight and cleared by immersion in 2% KOH for 6-8 h. Bones were stained with alizarin red (50 mg/L in 2% KOH) for 3-5 h. Skeletons were then cleared in 2% KOH and stored in 20% glycerol.

Mutation mapping and identification

Alx4^{m1Yzcm} heterozygotes of the B6 background were mated to D2 mice to generate F1 mice. Next, the F1 polydactylous mice were backcrossed to B6 mice to generate N2 mice. DNA samples of N2 polydactylous mice were prepared from tail samples by proteinase K digestion, phenol-chloroform extraction, and ethanol precipitation. DNA samples were screened for microsatellite markers by using polymerase chain reaction (PCR); PCR products were separated on 4% agarose gels by electrophoresis and analyzed.

The exons and the immediate flanking sequences of *Alx4* were amplified from *Alx4^{m1Yzcm}* heterozygotes and B6 genomic DNA. Primer sequences for *Alx4* are available on request. PCR products were purified and the sequences were read using the Big Dye Terminator v3.1 kit on an ABI-PRISM 3730.

Genotyping of mice

The point mutation introduced an *Hpy*F3I (*Dde*I) restriction site in *Alx4^{m1Yzcm}*. A 101-bp fragment that encompassed the point mutation was amplified from the genomic DNA by using a forward primer, 5'-TTCTAACCTTCTTTTCTCTTCCACA-3', and a reverse primer, 5'-CCCTGTCTCCTTCACACTGCG-3'. Digestion of the PCR product with *Hpy*F3I was predicted to yield DNA fragments of the following sizes: +/+ mice, 101 bp; +/- heterozygotes, 101, 29, and 72 bp; and -/- homozygous mice, 29 and 72 bp. Analysis after 4% gel electrophoresis revealed DNA bands of the expected sizes.

Reverse transcription (RT)-PCR

Total RNA was isolated from E12.5 embryos by using the TRIzol reagent (Invitrogen, Carlsbad, CA, USA). cDNA was synthesized using a RevertAid First Strand cDNA Synthesis Kit (Fermentas, EU) with oligo (dT)18 primers. RT-PCR for *Alx4* was performed using the following primers: forward: 5'-CACAACGCGGCCTTGCAG-3' and reverse: 5'-CCGTGCA TACACATCAGGGTAGT-3'. PCR conditions consisted of one cycle of denaturation for 5 min at 94°C, followed by 30 cycles of 30 s at 94°C, 30 s at 61°C, and 30 s at 72°C, and finally, one cycle of elongation for 5 min at 72°C. The PCR products were purified and sequenced.

Histology

Heterozygous *Alx4^{m1Yzcm}* mice were intercrossed and embryos at E19.5 were recovered, genotyped, fixed in 4% paraformaldehyde in phosphate-buffered saline, dehydrated, wax-embedded, sectioned to 6-μm thickness, and finally stained with Harris hematoxylin and eosin-Y stain.

RESULTS

Phenotypic characterization of *Alx4^{m1Yzcm}* heterozygous mice

Alx4^{m1Yzcm} mutants were originally isolated by ENU mutagenesis. They are character-

ized by alterations in the limb skeletal pattern, which lead to formation of a single extra digit (polydactyly) in the preaxial (anterior) part of one of the hindlimbs (rarely both) without a right-left side preference (Figure 1). Mutant mice were mated with B6 mice: 15 of the 71 progeny produced had the polydactylous phenotype, indicating a dominant mutation with incomplete penetrance.
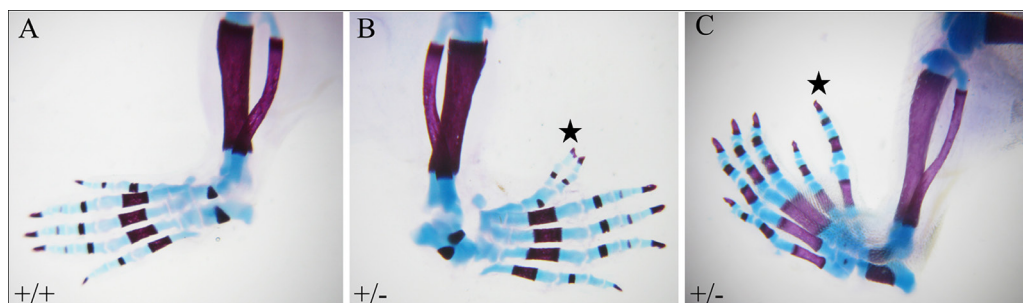

Figure 1. Preaxial polydactyly in *Alx4^m1Yzcm^* heterozygous mice. **A.** Wild-type mouse; **B.** and **C.** *Alx4^m1Yzcm^* heterozygous mice.

Polydactylous phenotype is caused by a nonsense mutation in the *Alx4* gene

For mapping, genomic DNA from N2 samples was analyzed with microsatellite markers across the whole genome. The mutation was mapped to mouse chromosome 2 between makers *D2Mit45* and *D2Mit184*, which are located at 50.63 and 53.07 cM, respectively. The observed recombinant ratio for both *D2Mit45* and *D2Mit184* was 6/81. The region between *D2Mit45* and *D2Mit184* contains the *Alx4* gene and the phenotypes of other *Alx4* mutants resemble that of the *Alx4^m1Yzcm^* mutant. Therefore, the *Alx4* gene was considered a good candidate for the *Alx4^m1Yzcm^* mutation.

On examination of the *Alx4* gene, a single nucleotide change - an A/T transversion (Figure 2A) - was observed in exon 2 of the *Alx4* gene at nucleotide position 433. This substitution converted the tyrosine codon to a lysine codon and generated a nonsense mutation at position 145 in the protein (Figure 2B). This point mutation introduced an *Hpy*F3I (*Dde*I) restriction site in *Alx4^m1Yzcm^*.

Sequencing of *Alx4* RT-PCR products from *Alx4^m1Yzcm^* heterozygous mutant mice showed that the mutant allele is transcribed, correctly spliced, and not subject to nonsense-mediated decay (Figure 2C). Translation of the mutant allele would produce a truncated protein.

Phenotypic characterization of the *Alx4^m1Yzcm^* homozygous mice

Homozygous mutants from *Alx4^m1Yzcm^* brother-sister matings were isolated, genotyped, and studied to characterize the *Alx4^m1Yzcm^* phenotype further. The majority of the homozygous mice was non-viable after birth and showed multiple abnormalities, including some homozygous mice exhibiting open eyelids at birth. Occasionally, some homozygous mice were viable and exhibited alopecia (Figure 3).
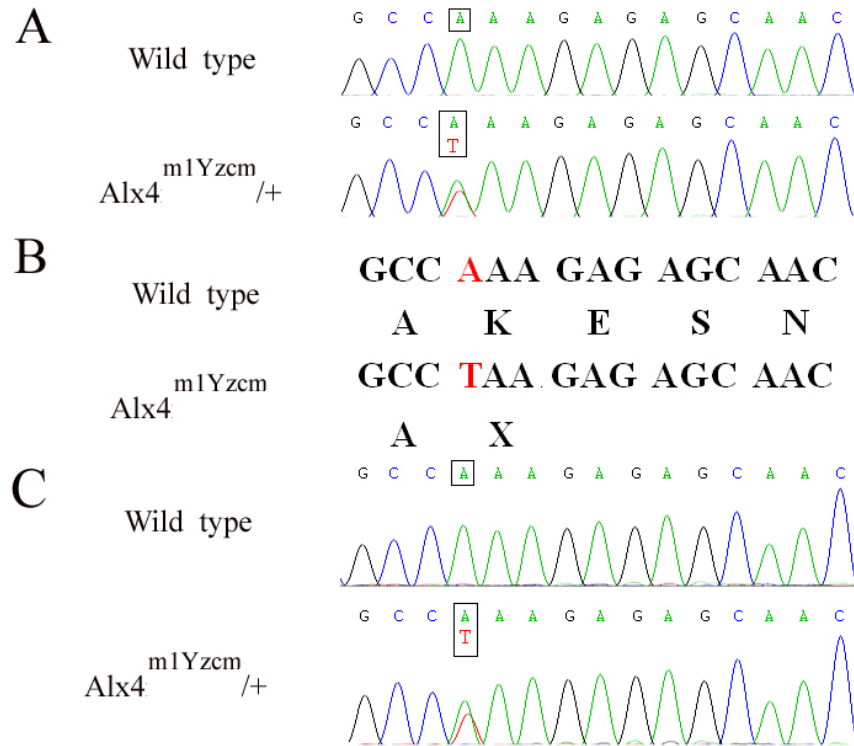
Figure 2. *Alx4* is mutated in *Alx4^m1Yzcm^* mice. **A.** Sequence analysis of the *Alx4* gene in *Alx4^m1Yzcm^* heterozygous mice by ABI-PRISM 3730; **B.** translation of wild-type and homozygous *Alx4^m1Yzcm^* alleles flanking the mutation site. The nucleotide mutated in the *Alx4^m1Yzcm^* allele is highlighted in red; **C.** sequence analysis of reverse transcription polymerase chain reaction products of *Alx4* in *Alx4^m1Yzcm^* heterozygous mice.
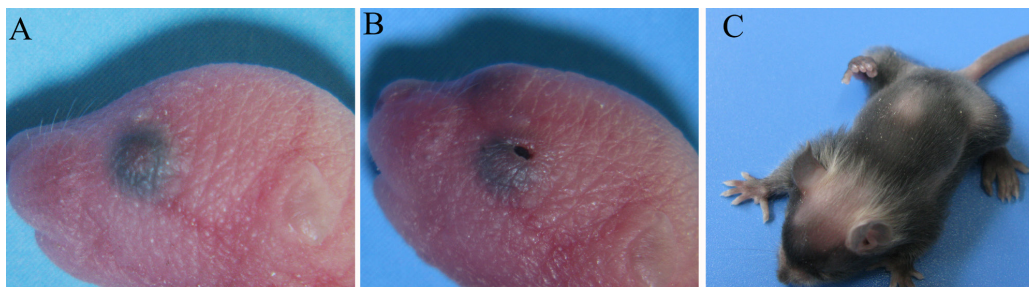

Figure 3. Open eyelids and alopecia in *Alx4^m1Yzcm^* homozygous mice. **A.** Wild-type mouse; **B.** eyelids open at birth in *Alx4^m1Yzcm^* homozygous mice; **C.** alopecia phenotype in *Alx4^m1Yzcm^* homozygous mice.

Alcian blue and alizarin red staining of homozygous mice showed extensive preaxial polydactyly of all 4 limbs (up to 7 digits), malformation (truncation) of the tibia (Figure 4), decreased size of the parietal bone, and loss of pubic bones (Figure 5).
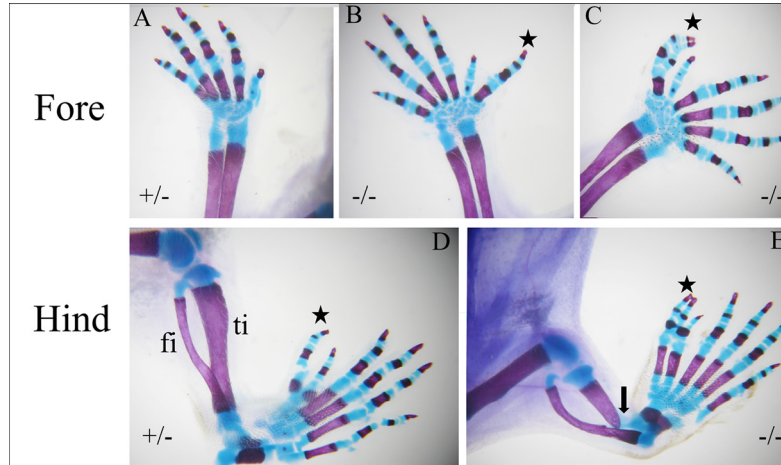
Figure 4. Preaxial polydactyly in *Alx4^m1Yzcm* homozygous mice. **A.** and **D.** *Alx4^m1Yzcm* heterozygous mice; **B.**, **C.** and **E.** *Alx4^m1Yzcm* homozygous mice. Top row = forelimbs; bottom row = hindlimbs. Stars = extra digit. Arrow = malformed (truncated) tibia. ti = tibia; fi = fibula.
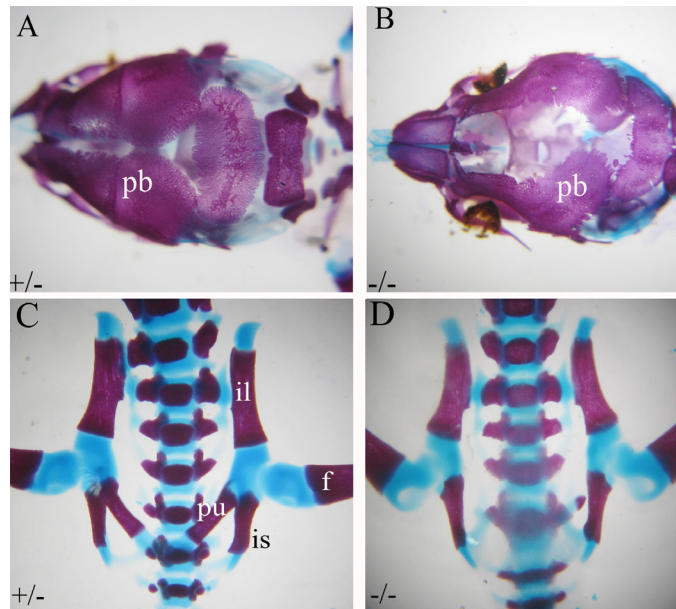

Figure 5. Decreased size of the parietal bone and loss of pubic bones in *Alx4^m1Yzcm* homozygous mice. **A.** and **C.** *Alx4^m1Yzcm* heterozygous mice; **B.** and **D.** *Alx4^m1Yzcm* homozygous mice. Note that, in the mutant, the parietal bone does not extend to the superior midline. pb = parietal bone; f = femur; il = iliac bone; is = ischial bone; pu = pubic bone.

Besides multiple skeletal abnormalities, defects were also detected in the ventral body wall, resulting in herniation of the abdominal contents. Histologic examination of embryos at E19.5 showed that the ventral abdominal wall musculature was absent and the skin was reduced in thickness in this region (Figure 6).
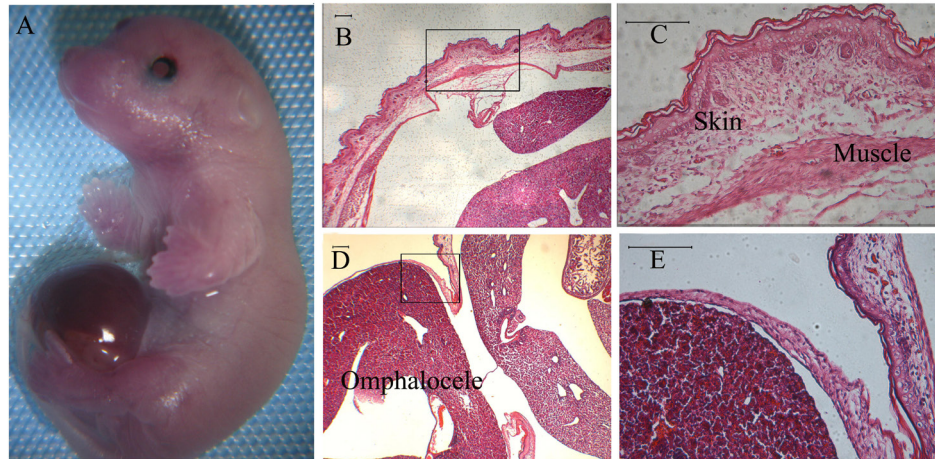
Figure 6. Omphalocele in *Alx4^{m1Yzcm}* homozygous mice. **A.** Appearance of an *Alx4^{m1Yzcm}* homozygous mice at E19.5. Note the presence of the liver and intestines outside the abdominal cavity. Note also the polydactyly visible on the hindlimb and forelimb; **B.-E.** Histologic analysis of the ventral abdominal wall of wild-type and *Alx4^{m1Yzcm}* homozygous mice. **B.** and **C.** Wild-type mice; **D.** and **E.** *Alx4^{m1Yzcm}* homozygous mice. Note the decreased thickness of both muscular and dermal layers in the mutant. Scale bars: 100 μm.

DISCUSSION

ENU is a chemical mutagen that mainly causes point mutations. Analysis of 62 sequenced germline mutations from 24 genes revealed that ENU predominantly modifies A/T base pairs, with 44% A/T to T/A transversions, 38% A/T to G/C transitions, and 8% G/C to A/T transitions, whereas other transitions and transversions each comprised 5% or less. Following translation into a protein product, these changes may result in 64% missense mutations, 10% nonsense, and 26% splicing errors (Justice et al., 1999; Wu et al., 2010). The *Alx4^{m1Yzcm}* mutation is an A to T transversion at nucleotide position 433 in the *Alx4* ORF. This mutation introduces a premature termination codon at residue 145. This indicates that the A to T mutation in *Alx4^{m1Yzcm}* is a common result of ENU mutagenesis.

The *Alx4* gene, which encodes a paired-type homeodomain protein that acts as a transcriptional regulator expressed in the anterior limb bud mesenchyme, plays an important role in limb patterning (Qu et al., 1997, 1998; Panman et al., 2005). *Alx4* loss-of-function mutations result in the *lst* mutant, a preaxial polydactylous phenotype with ectopic *Shh* expression in the anterior mesenchyme of the limb bud during development. Heterozygous mice show an extra digit on the anterior aspect of the hinddigit, whereas homozygous mice show a complex phenotype including extensive preaxial polydactyly of all 4 limbs (up to 9 digits), anomalies of the tibia, craniofacial defects, dorsal alopecia, weakness of the ventral body wall, and, in males, anomalies of the phallus and cryptorchidism (Forsthoefel, 1962, 1963; Qu et al., 1997, 1999). The phenotypic characterization of *Alx4^{m1Yzcm}* is very similar to that of *lst* mutants, although some differences are apparent. For example, in contrast to *lst* mutants, *Alx4^{m1Yzcm}* homozygotes have only preaxial digits (no more than 7). The basis of this difference is not clear.

An omphalocele is a major ventral body wall malformation characterized by a severe umbilical defect, with herniation of visceral organs covered by the peritoneum and amnion.

The frequency of this malformation is reported to be approximately 1 in 4000 live births (Matsumaru et al., 2011), and despite this high incidence, the cause of omphalocele formation remains unclear. In addition to *Alx4^{m1Yzcm}*, there are 5 mutations of *Alx4*: 3 chemically induced (*Alx4^{lst}*, *Alx4^{lst-Alb}*, *Alx4^{m1Btlr}*), 1 targeted (*Alx4^{tm1Rwi}*), and 1 spontaneous (*Alx4^{lst-J}*). The allelic series of mutations in the *Alx4* gene represents an extremely valuable genetic resource for elucidation of the mechanisms underlying omphalocele formation.

ACKNOWLEDGMENTS

REFERENCES

Büscher D, Grotewold L and Rüther U (1998). The *Xt^J* allele generates a *Gli*3 fusion transcript. *Mamm. Genome* 9: 676-678.

Catala M (2000). Control of the positioning of the vertebrate limb axes during development. *Morphologie* 84: 17-23.

Chen B, Li K, Zhang FL and Zhai GQ (2011). An ENU-induced mutation of *Nrg1* causes dilated pupils and a reduction in muscarinic receptors in the sphincter pupillae. *PLoS One* 6: e25176.

Forsthoefel PF (1962). Genetics and manifold effects of Strong's luxoid gene in the mouse, including its interactions with Green's luxoid and Carter's luxate genes. *J. Morphol.* 110: 391-420.

Forsthoefel PF (1963). The embryological development of the effects of strong's luxoid gene in the mouse. *J. Morphol.* 113: 427-451.

Hu J and He L (2008). Patterning mechanisms controlling digit development. *J. Genet. Genomics* 35: 517-524.

Justice MJ, Noveroske JK, Weber JS, Zheng B, et al. (1999). Mouse ENU mutagenesis. *Hum. Mol. Genet.* 8: 1955-1963.

Kuijper S, Feitsma H, Sheth R, Korving J, et al. (2005). Function and regulation of *Alx4* in limb development: complex genetic interactions with *Gli3* and *Shh. Dev. Biol.* 285: 533-544.

Matsumaru D, Haraguchi R, Miyagawa S, Motoyama J, et al. (2011). Genetic analysis of Hedgehog signaling in ventral body wall development and the onset of omphalocele formation. *PLoS One* 6: e16260.

Panman L, Drenth T, Tewelscher P, Zuniga A, et al. (2005). Genetic interaction of *Gli3* and *Alx4* during limb development. *Int. J. Dev. Biol.* 49: 443-448.

Qu S, Niswender KD, Ji Q, van der Meer R, et al. (1997). Polydactyly and ectopic ZPA formation in *Alx-4* mutant mice. *Development* 124: 3999-4008.

Qu S, Tucker SC, Ehrlich JS, Levorse JM, et al. (1998). Mutations in mouse Aristaless-like4 cause Strong's luxoid polydactyly. *Development* 125: 2711-2721.

Qu S, Tucker SC, Zhao Q, deCrombrugghe B, et al. (1999). Physical and genetic interactions between *Alx4* and *Cart1. Development* 126: 359-369.

Riddle RD, Johnson RL, Laufer E and Tabin C (1993). Sonic hedgehog mediates the polarizing activity of the ZPA. *Cell* 75: 1401-1416.

Tabin CJ and McMahon AP (2008). Developmental biology. Grasping limb patterning. *Science* 321: 350-352.

Takahashi M, Tamura K, Büscher D, Masuya H, et al. (1998). The role of *Alx-4* in the establishment of anteroposterior polarity during vertebrate limb development. *Development* 125: 4417-4425.

Wu BJ, Yin LJ, Yin HP, Ying XS, et al. (2010). A mutation in the *Kit* gene leads to novel gonadal phenotypes in both heterozygous and homozygous mice. *Hereditas* 147: 62-69.